

The COSAS survey I

First results from the IRAM mapping survey of ^{12}CO J=1-0 & J=2-1 emission in AGB and early post-AGB circumstellar envelopes.

J. Alcolea⁽¹⁾, A. Castro-Carrizo⁽²⁾ (P.I.), G. Quintana-Lacaci^(1,3), R. Neri⁽²⁾, V. Bujarrabal⁽¹⁾, F.L. Schöier⁽⁴⁾, J.M. Winters⁽²⁾, H. Olofsson⁽⁴⁾, M. Lindqvist⁽⁴⁾, R. Lucas⁽⁵⁾, and M. Grewing⁽²⁾

⁽¹⁾OAN (Spain), ⁽²⁾IRAM (France), ⁽³⁾IRAM (Spain), ⁽⁴⁾OSO (Sweden), ⁽⁵⁾ALMA (ESO)

ABSTRACT Here we present the first result from the COSAS (CO Survey of late AGB Stars) program (P.I. A. Castro-Carrizo), a J=1-0 and J=2-1 line emission mapping survey of a statistically representative sample of circumstellar envelopes around AGB and post-AGB stars. This mapping survey has been carried out to investigate the small and large scale morphological and kinematical properties of the molecular environment surrounding stars in the late AGB and early post-AGB phases. For this, COSAS ideally combines the high spatial resolution and sensitivity of the IRAM Plateau de Bure Interferometer, with the IRAM Pico de Veleta 30m-MRT capabilities to map more extended emission. The whole program includes of 45 stars, selected to sample a wide variety in mass loss rate, chemical type (M, S and C types), variability type (regular variables like Miras and OH/IRs, semiregulars, irregulars, and non varying post-AGBs), evolutionary state, and initial mass. By no means it is an unbiased sample, so results must be interpreted with care, and in terms of the different population of sources represented in the sample. COSAS products (at first, maps and velocity fields, and after modeling, excitation and density profiles across the envelopes) provides means to quantify variations in the mass-loss rate history, assess on the prevalence of different morphological and kinematical features, and investigate the appearance of fast aspherical winds in the late-AGB and early post-AGB phases. This paper, which is the first of a series of COSAS papers, presents the results from the final mapping of a sample of 16 selected sources (about 1/3 of the whole list), namely: WX Psc, IK Tau, TX Cam, RX Boo, X Her, CRL 2362, χ Cyg, V Cyg, S Cep, OH 104.9+2.4, R Cas, IRAS 19475+3119, IRAS 20028+3910, IRAS 21282+5050, IRAS 23321+6545 and CRL 2477. The envelopes around late AGB stars are found to be mostly spherical, but often presenting features like concentric arcs (R Cas and TX Cam), spiral density patterns (TX Cam), molecular high density patches testifying to highly irregular mass-loss process (WX Psc, IK Tau, V Cyg, and S Cep), and yet well-defined axis-symmetric morphologies and kinematical patterns (X Her and RX Boo). The molecular envelopes span a large range of sizes, from the relatively compact cases of CRL 2362, OH 104.9+2.4 and CRL 2477, to very large ones, such as in χ Cyg and TX Cam. Self-absorption features are observed in some cases, as in IK Tau and χ Cyg, testifying to the emergence of (aspherical?) winds in the innermost circumstellar regions. Strong axial structures with more or less complex morphologies are detected in four, out of five, early post-AGB stars of this first sub-sample (IRAS 20028+3910, IRAS 23321+6545, IRAS 19475+3119, and IRAS 21282+5050).

1: INTRODUCTION The study of the circumstellar shells around AGB and post-AGB sources, and of the mass loss responsible for them, is a fundamental key for the understanding of these late stages of the stellar evolution. At least during the AGB and early post-AGB phases, the best observational tool to study these envelopes is molecular spectroscopy. The COSAS program is designed to accurately map a sample of these envelopes in a variety of sources, by combining single-dish and interferometric observation of ^{12}CO in its two lowest rotational transitions: J=1-0 and 2-1. The target list consists in 45 sources, including regular variables, SRs, IRs and post-AGB sources, of different chemical composition (Ms, Cs, and S-type). Due to the large number of sources, we plan to publish the results in three papers. Here we only report on the outcome of the first 16 sources. The full list of targets in the program includes the following sources:

Regular variables: WX Psc, IK Tau, TX Cam, CRL 2362, χ Cyg, V Cyg, S Cep, R Cas, OH 104.9+2.4, R Gem, OH127.8+0.0, IRAS 06192+4657, R Leo, R LMi, CIT 6, R Hya, S CrB, V CrB, OH26.5+0.6, R Sct, W Aql, RR Aql, T Cep, LP And, CRL 2494 & CRL 3068.

Semiregular and irregular variables: RX Boo, X Her, IRC +50049, CRL 292, Betelgeuse, UU Aur, BM Gem, V Hya, RT Vir & TX Psc.

post-AGB sources: IRAS 19475+3119, IRAS 20028+3910, IRAS 21282+5050, IRAS 23321+6545, CRL 2477, He 3-1475, IRAS 19500-1709, IRAS 22223+4327 & OH 17.7-2.0. Sources in this first paper are underlined. Orange: O-rich sources; green: C-rich sources; blue: S-type sources.

2: OBSERVATIONS The ^{12}CO J=1-0 and 2-1 maps have been carried out with the IRAM Plateau de Bure Interferometer (PdBI) and 30m single-dish Millimeter Radio Telescope (30m-MRT). PdBI provides high spatial resolution data, better than 1" in the J=2-1 line, but due to limitations inherent to interferometry, can not provide information on structures larger than about 25" for the J=1-0 line (12" for the 2-1). This lost information can be recovered by combining the interferometric data with single dish observations. In the case of the IRAM telescopes, both instruments were designed to match this complementarity requirement, since the 30m-MRT can provide maps with resolution of 12" and 22" in the J=2-1 and 1-0 lines respectively, which fills very well the gap in the PdBI data. (In single dish maps, the limit on the largest detectable structure only comes from the size of the mapped region). This combination must be performed very carefully, paying special attention to the relative calibration between the two instruments, so no artificial features are produced. For very compact sources (< 6"-10"), smaller than the maximum spatial structure observable with the interferometer, just PdBI data are necessary. For slightly resolved out sources (with extents similar to the maximum size of the structures seen by the interferometer), PdBI maps were combined with 30m-MRT spectra taken at the center of the object, to recover the zero-space flux. For more extended sources, but still smaller than the primary beam of the individual antennas of the interferometer, PdBI data have been combined with 30m-MRT OTF observations to recover the flux at short spacings. Finally, for the more extended sources (larger than the primary beam on the PdBI), 30m-MRT OTF maps have been combined with PdBI mosaic maps (i.e. with several pointings) covering the full extent of the envelope. By using this procedure we have been able to measure the full extent of the molecular envelopes, at least in the J=1-0 line, in all sources but V Cyg (see Table 1).

3: RESULTS Here we present the maps from the first ~1/3 of sources (see Sect 1.). These results are summarized in the abstract, as well as in figures 1 to 5 and tables 1 and 2. Results for the rest of the sample, as well as detail modeling of some of the sources, will be presented in a series of forthcoming papers, still in preparation.

This work is based on observations carried out with the IRAM Plateau de Bure Interferometer and 30m-MRT. IRAM is supported by INSU/CNRS (France), MPG (Germany) and IGN (Spain). For further details on this poster see Castro-Carrizo et al. 2010, A&A, (in press).

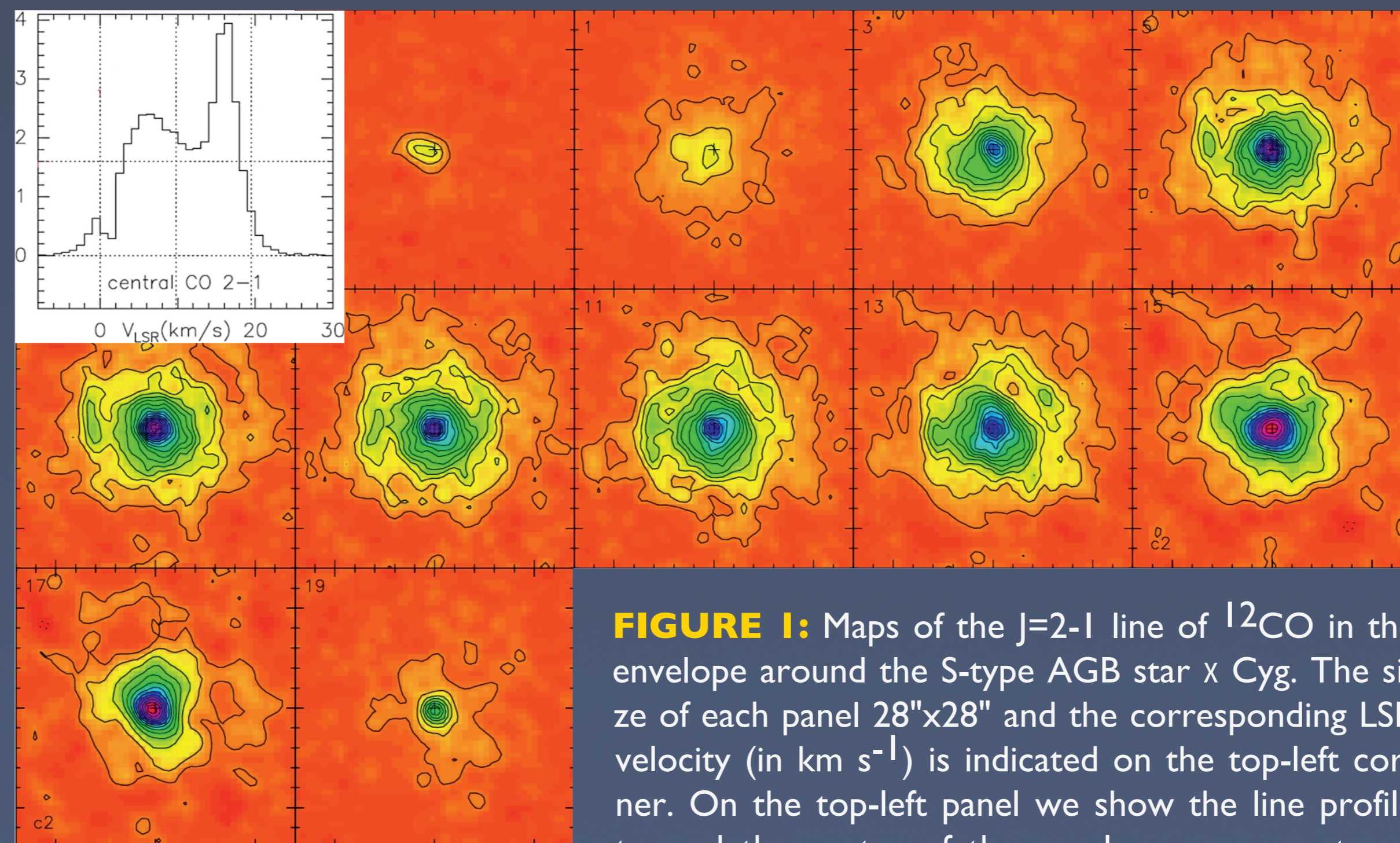


FIGURE 1: Maps of the J=2-1 line of ^{12}CO in the envelope around the S-type AGB star χ Cyg. The size of each panel 28"x28" and the corresponding LSR velocity (in km s^{-1}) is indicated on the top-left corner. On the top-left panel we show the line profile toward the center of the envelope, where a strong self absorption is detected at 2 km/s . A similar feature has been found in IK Tau. We speculate on the origin of this feature as result of faster winds (not necessary bipolar) arising at the center of the envelope.

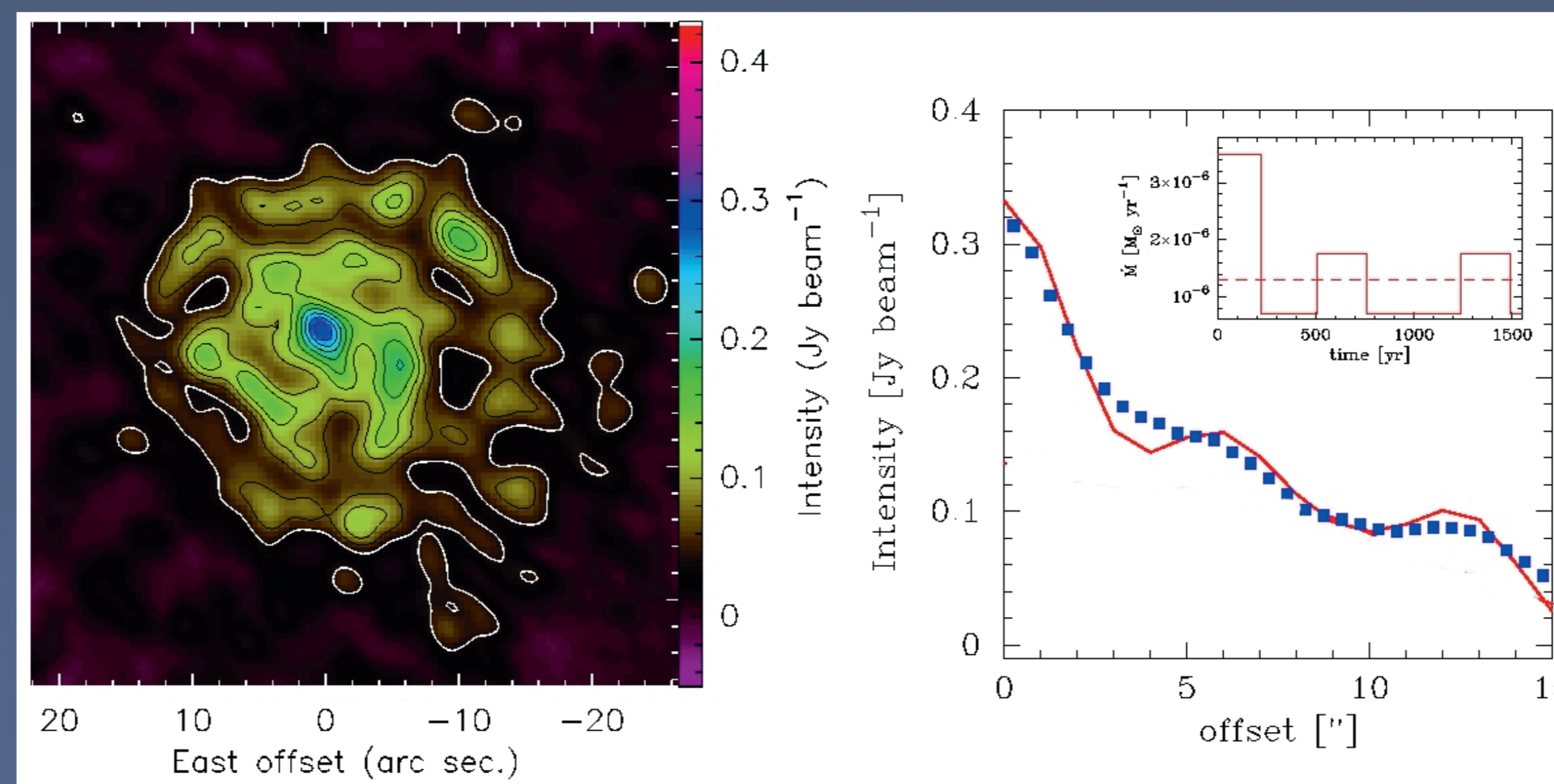


FIGURE 2: Variations in the mass loss rate detected in the envelope of the O-rich Mira R Cas. On the left, map of the ^{12}CO J=2-1 emission at the systemic velocity, displaying a two fragmented rings of enhanced emission. On the right, comparison of the azimuthal averaged radial profile of the line intensity (red line), with the predictions from a model where the mass loss rate varies with time (blue dots). The history of the mass loss in the model is shown in the upper-right inset.

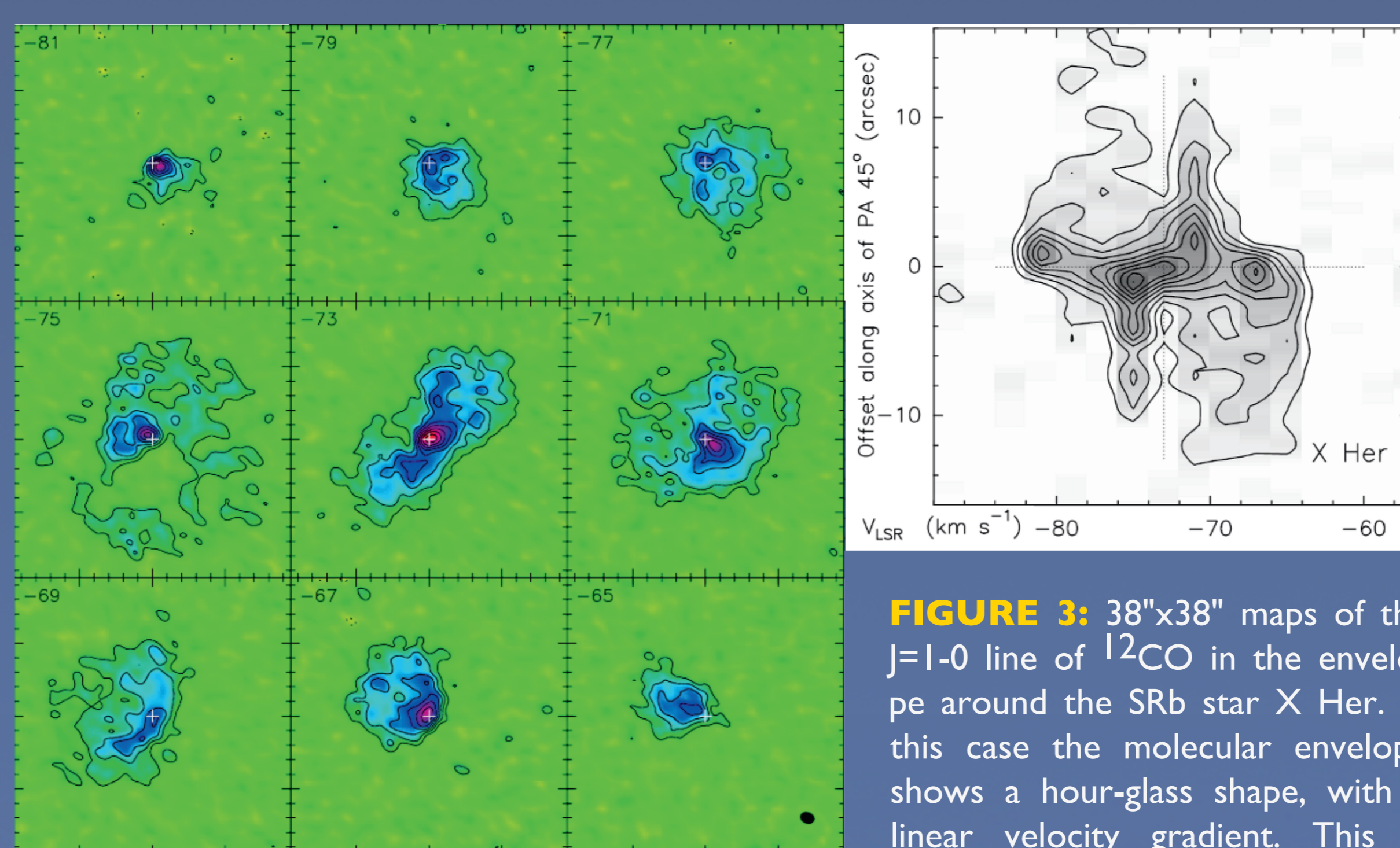


FIGURE 3: 38"x38" maps of the J=1-0 line of ^{12}CO in the envelope around the SRb star X Her. In this case the molecular envelope shows a hour-glass shape, with a linear velocity gradient. This is better display in the P-V diagram along the symmetry axis (at PA 45°) shown on the right. This structure and kinematics resembles those of the central parts of pPNe such as M1-92 or M2-56. A similar axis-symmetric shape is also found in the other SR in this 1st sub-sample, RX Boo. In this latter case the bipolar structure is located at the center of a rounded more extended halo.

TABLE 1: Sizes measured for the full extent of the envelopes that have been found round or slightly elongated at large scale. The sizes are convolved with the 30m-MRT mean beam (22" and 12" at J=1-0 and 2-1 respectively). CO photo-dissociation diameters using Mamon et al. (1988) formulation are also given.

source	^{12}CO J=1-0 CSE size	^{12}CO J=2-1 CSE size	photodiss. diameter
TX Cam	77"	69"	52"
V Cyg	≥90"	48"	39"
χ Cyg	97"	81"	76"
RX Boo	75"	52"	62"
S Cep	78"	48"	28"
R Cas	85"	65"	53"

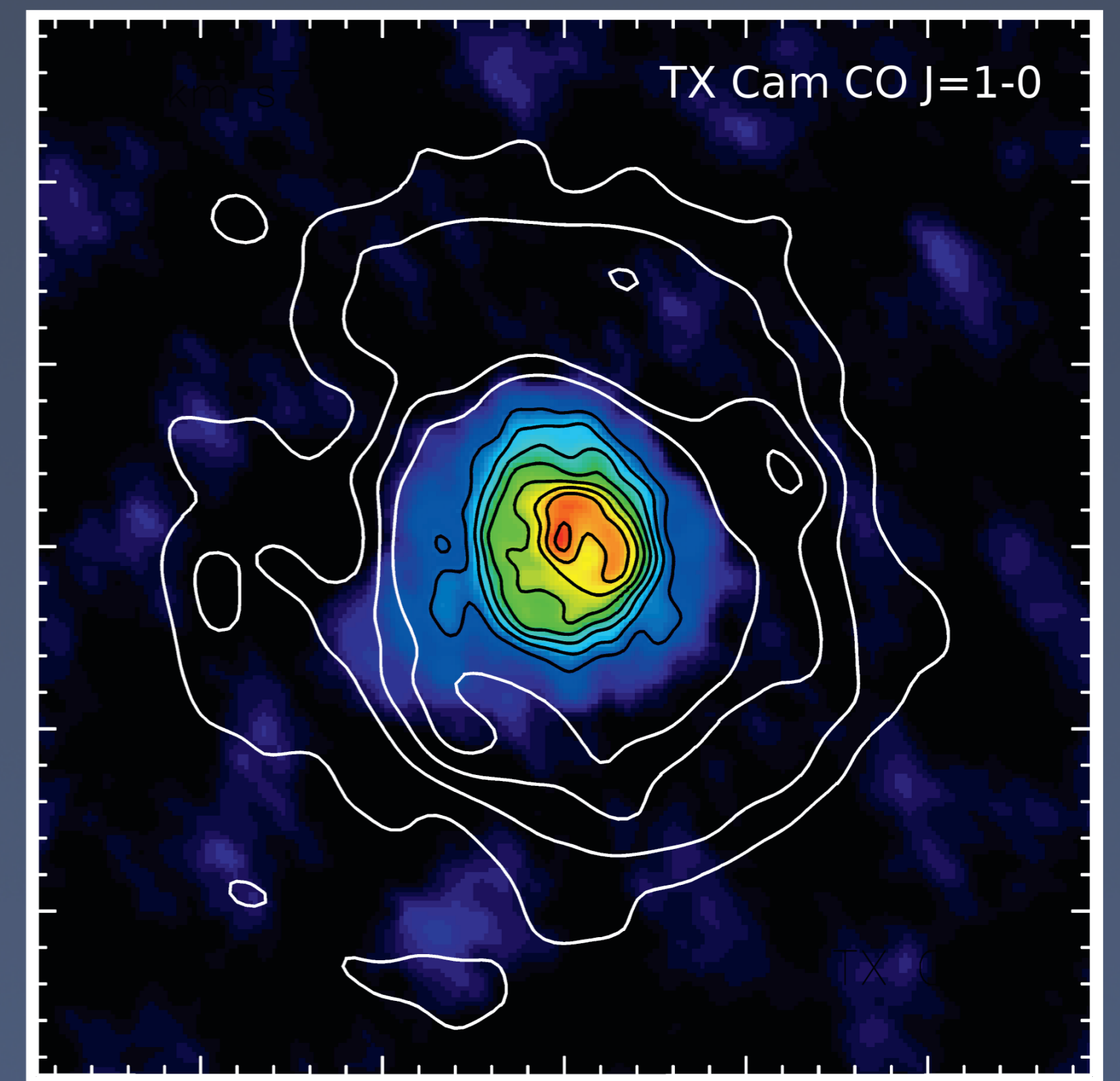


FIGURE 4: Montage of the J=1-0 (white contours, 5" resolution) and J=2-1 (black contours and false color image, 2" resolution) ^{12}CO emission in TX Cam at the systemic velocity. The panel size is 58"x58". The outer part of the envelope is nearly round, but a hooked structure (or a mini spiral) is detected at the center of the envelope. Such nested structures are often found in CSEs in our sample.

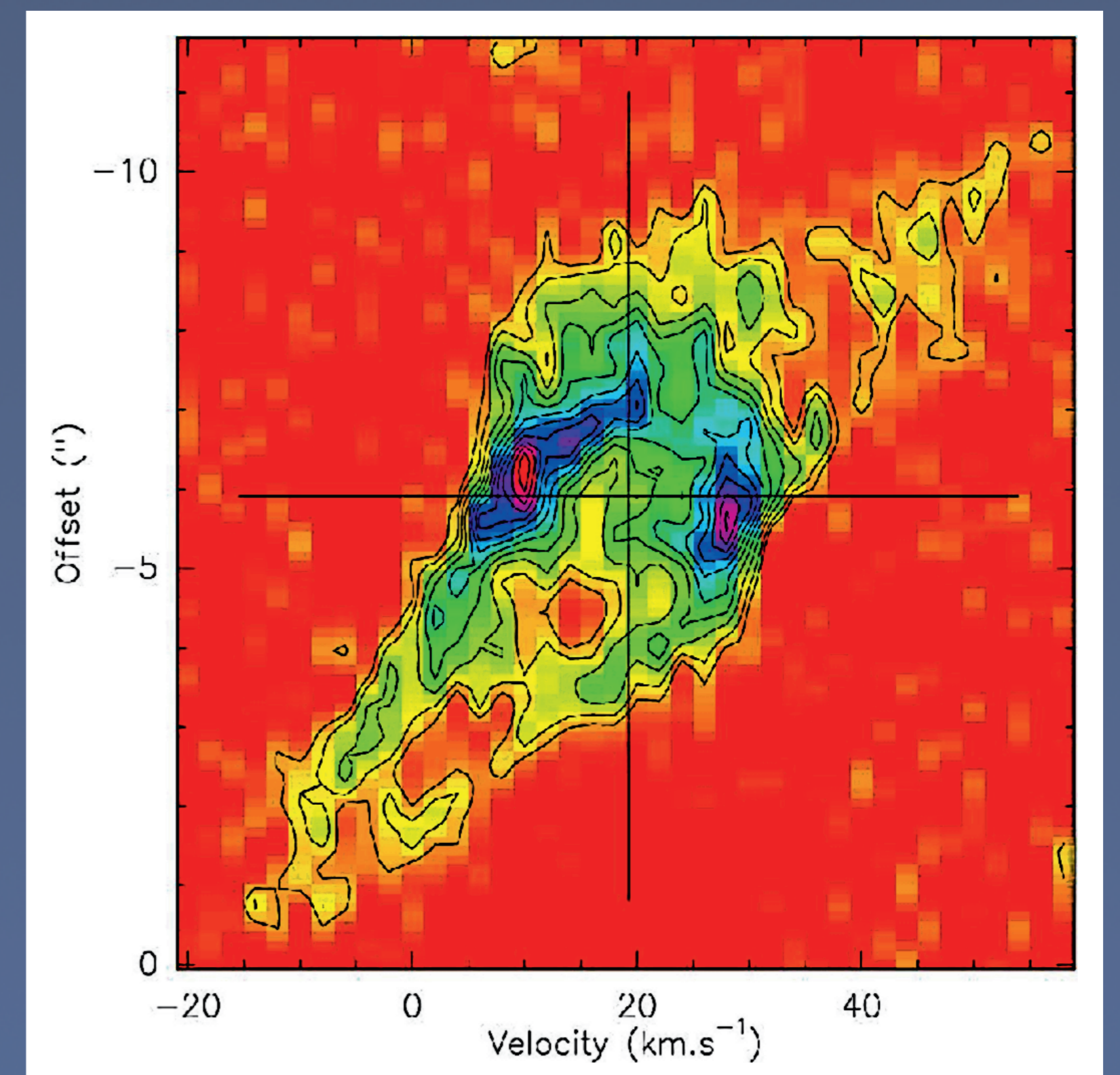


FIGURE 5: Position vs. Velocity diagram along the axis of symmetry of the pPN IRAS 19475+3119. This nebula displays a quadrupolar image in the optical, but in CO it shows a bipolar self-similar structure very much like the one of M1-92, except for the lack of the thick equatorial component.

TABLE 2: Summary of the morph-kinematical results in COSAS I. post-AGB sources are in red and SRs are in blue. Envelopes of regular variables appear round or slightly elongated at large scale, but show many features at small scales. The two SRs in the sample are peculiar (Fig. 3). All pPNe but one (where we lack of spatial resolution) show signatures of bipolarity at least in the innermost component.

source	innermost component	outermost component
WX Psc	rounded	aspherical
IK Tau	SHV aspher. winds	aspherical
TX Cam	spiral	spherical
RX Boo	P-V gradient	spherical
X Her	P-V gradient	no det. halo
CRL 2362	small	rounded
χ Cyg	SHV aspher. winds	spherical
V Cyg	rounded	aspherical
S Cep	aspherical	spherical
OH 104.9+2.4	small	rounded
R Cas	arc/spiral	spherical
IRAS 19475+3119	axial	bipolar flow
IRAS 20028+3910	SHVA winds	spherical
IRAS 21282+5050	axial	spherical
IRAS 23321+6545	SHVA winds	spherical
CRL 2477	small	rounded